Shared genetic basis for brain structure, insulin resistance and inflammation in schizophrenia: a colocalization study.

Amalie C. M. Couch[1*], Benjamin I. Perry[2], Edward R. Palmer[2], Jack Rogers[2], Rachel Upthegrove[1,2,3,4*]

[1] Department of Psychiatry, University of Oxford, UK.
[2] Institute for Mental Health, School of Psychology, University of Birmingham, Birmingham, UK.
[3] Birmingham Early Intervention Service, Birmingham and Solihull Mental Health Trust, UK.
[4] Oxford Health NHS Foundation Trust, UK.

***Joint Corresponding authors:**
Dr. Amalie Couch and Prof. Rachel Upthegrove,
Department of Psychiatry, University of Oxford,
Warneford Hospital, Oxford, OX3 7JX, United Kingdom

Tel: +44 (0) 1865 618200
Email: amalie.couch@psych.ox.ac.uk or rachel.upthegrove@psych.ox.ac.uk

KEYWORDS
Immuno-metabolic, psychosis, IL-6, multimorbidity, neurodevelopment, colocalization.

Abstract

Background: Psychotic disorders such as schizophrenia (SZ) are associated with structural brain changes and increased cardiometabolic disease risk, potentially linked through shared inflammatory mechanisms. However, whether these associations reflect shared genetic architecture remains unclear. We investigated genetic overlap between SZ, brain structure, insulin resistance (IR), and interleukin (IL)-6 signalling to uncover shared biological mechanisms.

Methods: We performed Bayesian multi-trait colocalization (HyPrColoc) analysis of SZ and validated markers of structural MRI (bilateral cortical thickness, grey matter volume), IR (TG:HDL-C ratio, fasting insulin), and IL-6 signalling (IL-6, IL-6R, IL-6ST), at 137 trait-associated SNPs (GWAS $p < 5\times10^{-8}$). *in silico* characterisation of candidate SNPs included protein (p)QTL gene set enrichment and developmental brain expression profiling in publicly available datasets.

Results: Primary analysis identified colocalization between SZ and at least one trait from brain structure, IR, or IL-6 signalling at 6 loci. After sensitivity analysis, the *SLC39A8* missense variant rs13107325 remained colocalized across SZ, bilateral cortical thickness, TG:HDL-C, and IL-6ST (PP_{coloc} = 0.93–0.99). SZ also colocalized with IL-6R at MHC-region variant rs2853986 (PP_{coloc} = 0.66–0.83). Pathway analysis of rs13107325 pQTLs revealed enrichment in synaptic development, glycan processing, and glycolysis pathways. Gene set enrichment highlighted links with coronary artery disease, myocardial infarction, and arteriosclerosis. SLC39A8 expression was enriched in cerebral vascular cells and increased during foetal and early postnatal brain development.

Conclusion: We identify shared genetic architecture between SZ, brain structure, IR, and inflammation at rs13107325. These findings underscore the importance of pleiotropic genetic effects in identifying new biological targets in psychosis.

Introduction

Individuals with schizophrenia (SZ) have 15-20 year shortened life expectancy, largely due elevated rates of metabolic and cardiovascular diseases. While these physical health conditions have traditionally been viewed as consequences of medication or lifestyle, growing evidence suggests they may reflect shared biological mechanisms, particularly chronic low-grade inflammation [1]. SZ itself is a highly heritable, polygenic disorder shaped by numerous common variants of small effect and rarer variants of larger effect [2], and it is possible that these have both central and peripheral effects, with impact on psychiatric and physical comorbidities reflecting their systemic nature.

Indeed, growing evidence suggests dysfunctional metabolism and inflammation are common pathological mechanisms across multiple organ systems, including the brain [3]. Evidence includes insulin resistance (IR) detectable in up to 40% of individuals at the onset of psychosis, prior to medication exposure [4–6] and increased low grade, chronic inflammation is prominently identified in unmedicated first-episode psychosis (FEP) [7–10]. Strongest evidence of the impact of chronic low level

inflammation ins SZ is related interleukin (IL)-6 a pleiotropic cytokine that signals through two distinct pathways: classical (cis) signalling, mediated by membrane-bound IL-6 receptor (IL-6R), and non-classical trans-signalling, when soluble (s)IL-6R engages the ubiquitously expressed co-receptor IL-6ST [11]. The relative contribution of cis- versus trans-signalling is modulated by the ratio of IL-6R to IL-6ST expression [12,13]. The co-occurrence of SZ, inflammation and metabolic dysfunction highlights the relevance of profiling plasma IL-6, IL-6R, and IL-6ST to investigate whether shifts in IL-6 signalling, particularly trans-signalling, contribute to metabolic comorbidities in psychosis through shared immuno-metabolic mechanisms.

Robust evidence demonstrates changes to brain structure in individuals with SZ. Structural magnetic resonance imaging (sMRI) in individuals with SZ implicate cortical thinning [14] and decreased grey matter volume (GMV) [15], present from before illness onset. SZ and cortical thickness (CT) share an overlap of genomic loci that are enriched for nervous system development, apoptosis, cell communication [16] and immunological signatures [17]. Furthermore, genetically predicted levels of IL-6 have been previously linked with changes to GMV and CT [18]. Brain structure is both heritable and shaped during development [19], and many models of SZ suggest that genetic risk influences brain maturation with impacts revealed in late adolescence and early adulthood with the onset of psychosis. Human studies and animal models suggest that prenatal immune exposure [20–24], driven by elevated IL-6, impacts brain development and increases susceptibility to psychosis in adulthood.

We extend these current hypotheses by proposing that specific risk loci may have pleiotropic effects on brain developmental processes, metabolism and inflammation during early development that prime risk for psychosis and multimorbidity. To investigate this hypothesis, we applied hypothesis prioritisation for multi-trait colocalization (HyPrColoc), a Bayesian method for identifying shared causal variants across traits that moves beyond genome-wide correlations to identify specific loci where genetic variation may simultaneously impact systems. We investigated colocalization among genetic loci implicated in SZ, brain structure (bilateral CT and normalised GMV); IR (triglyceride:HDL-

cholesterol [TG:HDL-C] and fasting insulin [FI]), and IL-6 signalling (IL-6, IL-6R, IL-6ST). Uncovering such converging risk loci offers the potential to identify shared mechanisms and novel treatments in psychosis multimorbidity.

Methods

Summary Statistics for Schizophrenia, Brain Structure, Insulin Resistance and IL-6 Signalling-related Traits

For SZ, we used publicly available summary data from the most recent Psychiatric Genomics Consortium (PGC) GWAS (76,755 cases and 243,649 controls)[25]. We also used publicly available summary GWAS data from large-scale consortia (Table 1) for 8 well characterised traits: three structural MRI phenotypes (left hemisphere cortical thickness [LH-CT], right hemisphere cortical thickness [RH-CT], and normalised grey matter volume [GMV] for head size)[26]; two biomarkers of IR (TG:HDL-C and fasting insulin [FI] adjusted for BMI) [27,28] and three IL-6 signalling proteins (IL-6, IL-6R, and IL-6ST)[29]. All GWAS were conducted in European adult samples and adjusted for population stratification, age, and sex. Ethical approval was obtained by the original GWAS authors in accordance with the protocols of each individual study.

Table 1: *Summary GWAS statistics used for schizophrenia, structural MRI (sMRI), biomarkers of insulin resistance and IL-6 signalling in plasma. PGC = Psychiatric Genomics Consortium; UKBB = UK Biobank; MAGIC = Meta-Analyses of Glucose and Insulin-related traits Consortium; sMRI = structural magnetic resonance imaging.*

Trait Group	Trait	Consortium	Author, Year	Sample Size	Case / Controls	Participant Description
Schizophrenia	Schizophrenia (SZ)	PGC	Trubetskoy, 2022[25]	320,404	76,755 / 243,649	European Adults
sMRI	Left Mean Global Cortical Thickness (LH-CT)	UKBB	Smith, 2021[26]	22,138	-	European Adults
	Right Mean Global Cortical Thickness (RH-CT)					
	Grey Matter Volume					

	Normalised for Head Size (GMV)					
Biomarkers of Insulin Resistance	Triglyceride:High Density Lipoprotein Cholesterol (TG:HDL-C)	UKBB	Oliveri, 2024[27]	402,398	-	European Adults
	Fasting Insulin adjusted for BMI (FI)	MAGIC	Lotta, 2017[28]	108,557	-	European Adults
IL-6 Signalling	IL-6	UKBB	Sun, 2023[29]	54,219	-	European Adults
	IL-6R					
	IL-6ST					

Multi-trait colocalization

We employed hypothesis prioritisation for multi-trait colocalization (HyPrColoc) [30] to identify shared genomic region risk loci see (Figure 1). Using Bayesian statistics, HyPrColoc (R package *jrs95/hyprcoloc*, version 0.0.2) estimates the posterior probability that multiple traits share a single causal SNPs by evaluating possible causal configurations, thereby identifying a "candidate variant", without delineating direction of association.

We first identified 137 lead index SNPs that demonstrated Bonferroni-significant evidence of locus-level correlation (GWAS $p < 5\times10^{-8}$) with brain structure, IR or IL-6 signalling-related traits. To quantify colocalization of each trait, we generated "lookup tables" in python (version 3.9.6) that included all SNPs located within ±500 kb of the lead index SNP. HyPrColoc was subsequently run in R (version 4.4.3) to detect shared genetic risk loci among trait clusters that included SZ.

In Bayesian terms, $prior_1$ reflects the probability that at least one trait has a causal variant in the region, while $prior_2$ represents the probability that a causal variant is associated with more than one trait. The regional and alignment thresholds specify how closely association signals must overlap spatially and in pattern to be considered colocalised, thereby refining confidence in shared causal variants. Therefore, our primary analysis used the default variant-specific prior settings ($prior_1 = 1x10^{-4}$; $prior_2 = 0.05$) and regional and alignment thresholds (both set to 0.5).

Sensitivity Analysis and Visualisation

Using a Bayesian framework allows us to formally incorporate prior knowledge and quantify the strength of evidence for shared genetic signals across traits by varying $prior_2$, regional and alignment thresholds, thereby enhancing the interpretability. Therefore, to evaluate the robustness of colocalization signals and cluster stability, we repeated the analysis using both increasingly stringent $prior_2$ values (0.05, 0.02, 0.01, 0.005, 0.001) and increasingly stringent regional and alignment thresholds (0.5, 0.6, 0.7, 0.8, 0.9).

To visualise cluster stability across these permutations, heatmaps were generated based on a similarity matrix between clusters. Where evidence for potential colocalization was found, stacked regional association plots were produced to visually inspect the candidate SNPs, forest plots to identify the strength of their associations across each trait, and the local linkage disequilibrium (LD) structure within the genomic region.

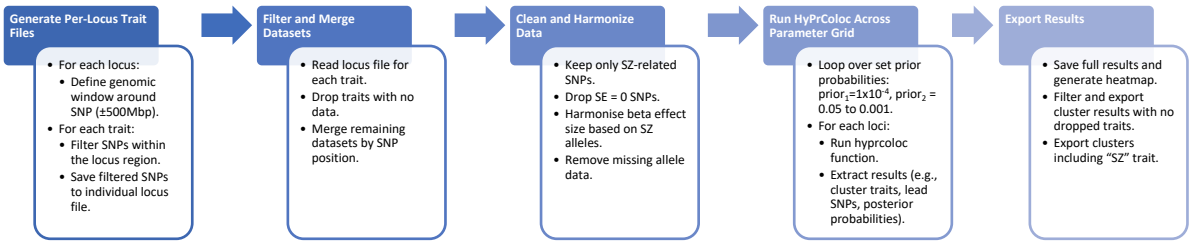

Figure 1: *Schematic of HyPrColoc[30] process applied in this study.*

Functional Characterisation in Silico of Candidate SNPs

Quantitative Trait Loci Analysis

To investigate the functional impact of candidate SNPs that colocalized SZ with brain structure, insulin resistance and inflammation traits, we performed quantitative trait loci (QTL) analyses focusing on expression QTLs (eQTLs) and protein QTLs (pQTLs). Data for eQTL were sourced from the GTEx

Portal (version 8), encompassing tissue-specific genetic associations with gene expression across diverse human tissues. Correlation of eQTLs with trait risk SNPs (GWAS $p < 5x10^{-8}$) was carried out using the *eQTpLot* package (version 0.0.0.9). Linkage disequilibrium (LD) information was incorporated to account for correlated variants ($R^2 \geq 0.5$). pQTL data were obtained from the UK Biobank Pharma Proteomics Project (UKB-PPP), which uses aptamer-based proteomic profiling of circulating protein levels in approximately 50,000 individuals from the UK Biobank [29]. Up- and down-regulated pQTLs (association $p < 1.7x10^{-11}$) were extracted for subsequent pathway analyses.

Pathway Enrichment Analysis

To characterise biological pathways linked to SNP-associated pQTLs, we then conducted enrichment analyses using the *EnrichR* package (version 3.4). Over-representation analysis (ORA) was performed separately for proteins exhibiting increased or decreased expression correlated with the minor allele. Gene Ontology (GO) Biological Process and Kyoto Encyclopaedia of Genes and Genomes (KEGG) pathway databases were used for annotation. Enrichment significance was assessed using gene ratio metrics and adjusted p-values using the BH method, then sub-setting the top 10 significant pathways (FDR < 5%, ranked by Fold Enrichment). Additionally, gene set enrichment analysis (GSEA) was carried out on a ranked list of all pQTL-associated genes. GSEA employed three curated databases: DisGeNET (gene-disease associations) and MSigDB Hallmark (50 canonical gene sets). Statistical significance in GSEA was evaluated using odds ratios and adjusted p-values, with significant gene sets (BH correction FDR < 5%) plotted.

Expression Profiling in RNA Sequencing Datasets

To examine the developmental expression pattern of genes implicated at colocalised loci, we also analysed three publicly available transcriptomic datasets of the developing human brain. First, single-cell RNA sequencing data from Wang et al. (2025) were interrogated to assess gene expression across annotated cell populations in the developing human cortex at multiple stages during development, including vascular cells, glia, and neuronal subtypes [31]. Second, using the Gene Expression in Cortical

Organoids (GECO) online tool, time-course bulk RNA-seq data from Gordon et al. (2021) of human cortical organoids were used to evaluate gene expression during in vitro differentiation [32,33]. Third, likewise using the GECO tool, bulk RNA-seq data from the BrainSpan Atlas of the Developing Human Brain were extracted [33], spanning prenatal to adulthood stages (8 post-conception weeks to 40 years).

Results

Multi-trait Colocalization between schizophrenia, cortical structure, biomarkers of insulin resistance and IL-6 signalling.

Primary Analysis

Under default prior thresholds, primary analysis identified 5 traits that clustered with SZ at 6 distinct genetic loci (Table 2):

- SZ colocalises with brain structure at the intronic variant rs3820822 (LH- and RH-CT; posterior probability for colocalization (PP_{coloc}) = 0.408).
- SZ colocalises and insulin resistance at two intronic variants: rs6765484 (TG:HDL; PP_{coloc} = 0.7463) and rs881844 (TG:HDL; PP_{coloc} = 0.6782).
- SZ colocalises with IL-6 signalling at the intergenic variant rs2853986 (IL-6R; PP_{coloc} = 0.8282).
- SZ colocalised with brain structure, insulin resistance and IL-6 signalling at two loci: the missense variant rs13107325 (IL6ST, TG:HDL-C, CT and GMV; PP_{coloc} = 0.4549 which increased substantially following the drop-out of GMV – see sensitivity analysis section), and the intergenic variant rs4240624 (IL6ST, FI and LH-CT; PP_{coloc} = 0.3571).

None of the 6 colocalising candidate variants (Table 2) are in linkage disequilibrium (LD) with significant GWAS index SZ SNPs, except for rs13107325 which is an index SNP for SZ.

Table 2: *Results from primary colocalization Bayesian analysis, tabulating unique candidate SNPs clustering traits with SZ at default settings ($prior_1 = 1x10^{-4}$, $prior_2 = 0.05$, alignment and regional thresholds = 0.5). Minor allele frequency (MAF) of*

*the candidate SNP was derived from European reference population via LDLink. PP_{coloc} represents the posterior probability that a single shared causal SNP amongst traits. $PP_{explained}$ represents the amount of variance amongst the shared traits is explained by the candidate SNP. N SNPs are the number of SNPs present in all trait datasets compared. †SNP is an index SNP for schizophrenia with an association $p < 5x10^{-8}$. * PP_{coloc} increased to >0.90 in sensitivity analysis after GMV was dropped from the cluster with increasing regional and alignment thresholds (see Sensitivity Analysis).*

Candidate SNP	**Cytogenetic $Region_{candidate}$**	**$MAF_{candidate}$**	**Gene Implicated**	**Variant Type**	**Colocalised Traits with SZ**	**PP_{coloc}**	**$PP_{explained}$**	**N SNPs**
rs3820822	2p23.3	0.3787	DPYSL5	Intron	LH-CT, RH-CT	0.408	0.044	1368
rs6765484	3p21.31	0.4871	RBM6	Intron	TG:HDL-C	0.7463	0.0361	9156
rs881844	17q12	0.3320	STARD3	Intron	TG:HDL-C	0.6782	0.276	660
rs2853986	6p21.33	0.0855	RNU6-283P, FGFR3P1	Intergenic	IL-6R	0.8282	0.1438	54615
rs4240624	8p23.1	0.0746	PPP1R3B-DT	Intergenic	IL6ST, FI, LH-CT	0.3571	0.3732	37917
rs13107325†	4q24	0.0795	SLC39A8	Missense	IL-6ST, TG:HDL-C, LH-CT, RH-CT, GMV	0.4549*	1.0000	10113

Sensitivity Analysis

As the stringency of $prior_2$, alignment, and regional thresholds increased, each trait cluster consistently identified the same top candidate colocalised variant as under the default settings (Figure 2). First, the trait cluster that colocalised at the candidate variant of rs13107325 demonstrated the greatest robustness (PP_{coloc} = 0.93–0.99) after GMV trait was dropped (required alignment and regional thresholds < 0.6), maintaining colocalization between SZ, brain structure traits (LH/RH-CT) and IR (TG:HDL-C). This was the case even under the most stringent conditions (thresholds up to 0.9) and with $prior_2$ as low as 1×10^{-4} (Figure 2). Inclusion of the IL-6ST trait within this cluster required a less stringent $prior_2$ threshold ($\geq 5\times10^{-3}$).

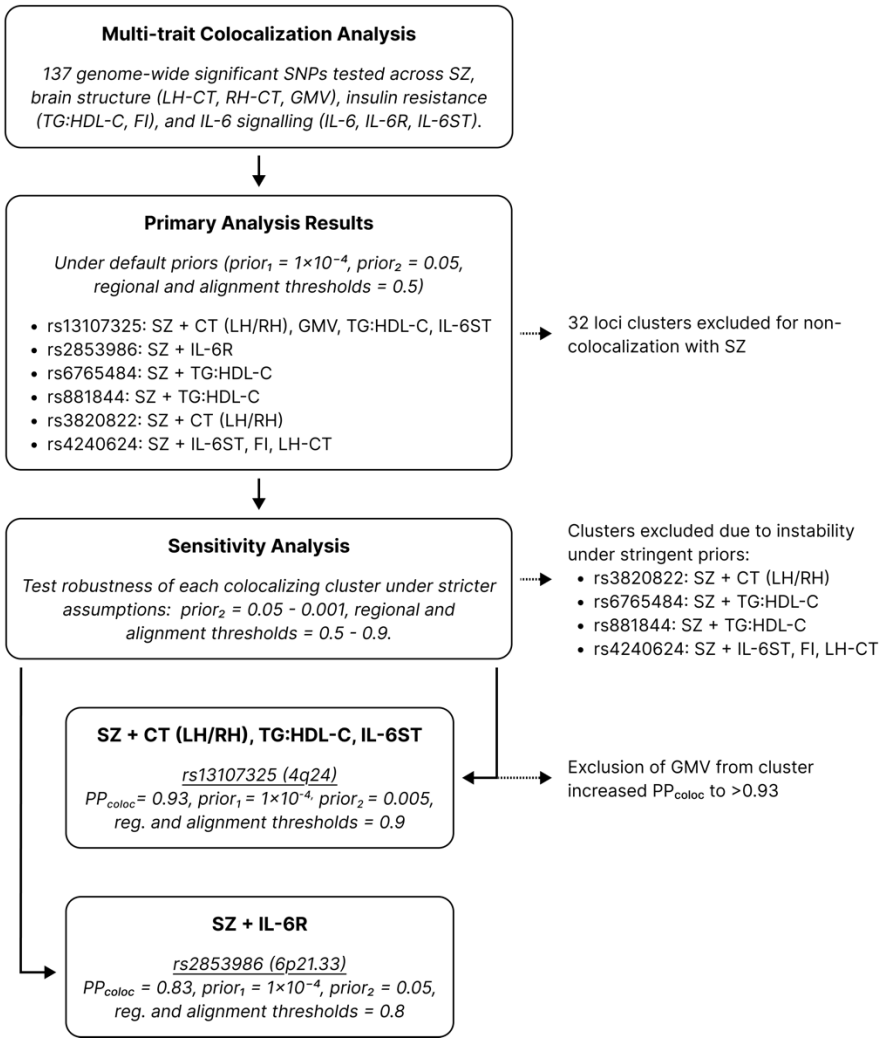

Figure 2: *Prioritisation workflow for multi-trait colocalization analysis between schizophrenia, brain structure, biomarkers of insulin and IL-6 signalling traits. A total of 137 genome-wide significant SNPs were tested across schizophrenia (SZ), brain structure (LH-CT, RH-CT, GMV), insulin resistance (TG:HDL-C, FI), and IL-6 signalling (IL-6, IL-6R, IL-6ST) using HyPrColoc. Primary analysis under default priors identified six loci showing colocalization with SZ. An additional 32 clusters of traits were excluded due to lack of colocalization with SZ. Sensitivity analysis was performed to test cluster robustness under increasingly stringent* $prior_2$*, regional (reg.), and alignment thresholds. 4 clusters (rs3820822, rs6765484, rs881844, rs4240624) were excluded due to instability. The rs13107325 cluster demonstrated the strongest and most consistent colocalization with SZ across all domains after exclusion of GMV, while rs2853986 (IL-6R) also retained moderate robustness.*

Next, the SZ and IL-6R cluster demonstrated the second strongest robustness in sensitivity analysis (Figure 2). For this cluster, the candidate variant was consistently rs2853986, with PP_{coloc} = 0.83 across recommended $prior_2$ = 0.05, and regional/alignment thresholds = 0.5–0.8. At a lower $prior_2$ = 0.02, the PP_{coloc} decreased to 0.66, but the candidate variant remained rs2853986.

Following this, rs6765484 and rs881844 candidate SNP clusters (both TG:HDL-C with SZ; PP_{coloc} = 0.43-0.75) persisted only under recommended $prior_2$ = 0.05 and moderate thresholds (0.5-0.7) and were therefore excluded from further analysis (Figure 2). Finally, the clusters of SZ with IL-6ST, FI, LH-CT at rs4240624, and SZ with LH-CT and RH-CT at rs3820822 were unstable past default thresholds, and only existed at $prior_1 = 1x10^{-4}$, $prior_2$ = 0.05 and alignment/regional thresholds = 0.5, and were likewise excluded from further analysis (Figure 2).

Characterisation of rs13107325

As the only stable and most robust cluster to encompass brain structure, insulin resistance, and IL-6 signalling traits colocalizing with schizophrenia (Figure 3), rs13107325 was selected for in silico functional characterisation. rs13107325 (C/T, p.Ala391Thr) is a well-characterised missense mutation in *SLC39A8*, first attributed to schizophrenia risk in 2012 by Carrera et al. [34]. *SLC39A8* encodes a divalent metal ion transporter (also known as ZIP8) responsible for the transport of essential cations such as manganese and zinc across plasma membranes [35]. The Ala391Thr substitution caused by rs13107325 results in partial loss of transporter function, disrupting intracellular metal homeostasis and potentially influencing downstream cellular processes [35]. To explore its regulatory and biological impact, we examined expression and protein quantitative trait loci (eQTL and pQTL) effects.

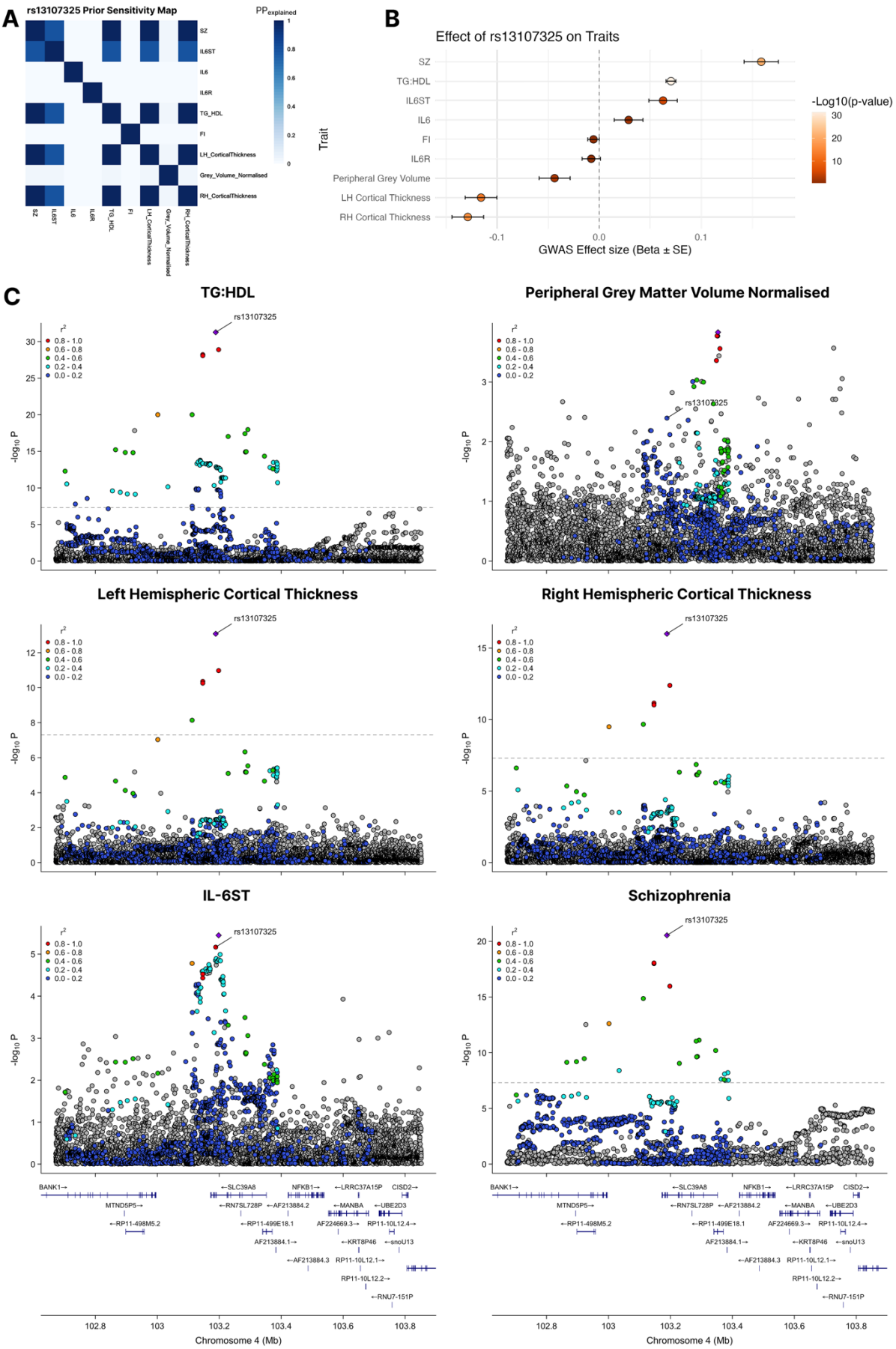
A
rs13107325 Prior Sensitivity Map
PP explained
SZ
IL6ST
IL6
IL6R
TG_HDL
FI
LH_CorticalThickness
Grey_Volume_Normalised
RH_CorticalThickness
B
Effect of rs13107325 on Traits
Trait
SZ
TG:HDL
IL6ST
IL6
FI
IL6R
Peripheral Grey Volume
LH Cortical Thickness
RH Cortical Thickness
-Log10(p-value)
GWAS Effect size (Beta ± SE)
C
TG:HDL
Peripheral Grey Matter Volume Normalised
Left Hemispheric Cortical Thickness
Right Hemispheric Cortical Thickness
IL-6ST
Schizophrenia
rs13107325
r2
0.8 - 1.0
0.6 - 0.8
0.4 - 0.6
0.2 - 0.4
0.0 - 0.2
-log10 P
Chromosome 4 (Mb)

Figure 3: *(A) Sensitivity plot of candidate SNP rs13107325 across all traits, demonstrating repeated calls of the hyprcoloc function to compute a similarity matrix which illustrates how strongly clustered/colocalized pairs of traits are across different input thresholds and priors. The darker the blue, the more robust colocalization of trait pairs is found to be in sensitivity analyses. (B) Variant Effect Size forest plot in all traits used in the study, data from GWAS studies laid out in Table 1. (C) Regional genetic association plots for the most robust colocalised loci returning evidence for colocalization between schizophrenia, brain structure, insulin resistance and IL-6 signalling. Regional association plots denote chromosomal location (x axis) and strength of association with listed trait (−log10(p)) (y axis) alongside genomic position. SNP r^2 estimated from the European panel from 1000 Genomes cohort.*

In GTEx, rs13107325 was significantly associated with increased expression of *PABPC1P7* in the cerebellum ($p = 1.93 \times 10^{-4}$, normalized effect size = 0.62). While *PABPC1P7* itself is a pseudogene with limited functional annotation, members of the *PABPC1* gene family are known to regulate mRNA translation and stability. rs13107325 was not identified as a significant eQTL for *SLC39A8* in any tissue available on GTEx. Moreover, there was no enrichment of *SLC39A8*-related eQTLs in GWAS-significant loci in SZ (P-P plot correlation of P_{GWAS} with P_{eQTL}: p = 0.774, r^2 = -0.08; Supplementary Figure 1), suggesting that the effects of rs13107325 are primarily driven by the loss of *SLC39A8* transporter function in SZ, rather than differential expression [35].

In contrast, pQTL analysis identified 64 proteins significantly ($P < 1.7x10^{-11}$) associated with rs13107325 (Supplementary Figure 2). Over-representation analysis of these proteins among biological processes revealed functional enrichment for pathways relevant to brain and synaptic development, and processing of o-linked glycans (Figure 4A). The 53 pQTLs upregulated in carriers of the rs13107325 minor allele were enriched for gene ontology (GO) terms including regulation of pre-synapse (fold enrichment [FE] = 30.43, p-adjusted = 0.0179) and synapse (FE = 10.87, p-adjusted = 0.0179) assembly, regulation of nervous system development (FE = 6.31, p-adjusted = 0.0112). KEGG pathway analysis further implicated cell adhesion molecules (FE = 15.52, p-adjusted = $8.40x10^{-6}$), ECM-receptor interactions (FE = 11.95, p-adjusted = $3.45x10^{-2}$), HIF-1 (FE = 9.67, p-adjusted = $3.45x10^{-2}$), Ras (FE = 5.96, p-adjusted = $3.45x10^{-2}$) and PI3K-AKT signalling pathways (FE = 4.89, p-adjusted = $3.45x10^{-2}$). Conversely, the 11 downregulated pQTLs were enriched for O-glycan processing in GO

analysis (FE = 105.48, p-adjusted = 0.045) and O-glycan biosynthesis pathways (mucin type: FE = 82.09, p-adjusted = 3.66×10^{-3}; other type: FE = 4.89, p-adjusted = 3.66×10^{-3}) in KEGG analysis (Figure 4A).

Gene set enrichment analysis (GSEA) of all 63 pQTLs in MSigDB Hallmark and DisGeNET gene sets (Figure 4B) identified enrichment for angiogenesis (Odds ratio [OR] = 29.66, p-adjusted = 0.004) and glycolysis (OR = 6.71, p-adjusted = 0.024), as well as cardiometabolic disorders such as coronary artery disease (OR = 4.99, p-adjusted = 2.27×10^{-3}), myocardial infarction (OR = 4.59, p-adjusted = 7.33×10^{-3}) and arteriosclerosis (OR = 4.05, p-adjusted = 0.02).

To determine the spatiotemporal context in which rs13107325 may exert its effects during development, we examined *SLC39A8* expression in publicly available single-cell RNA sequencing datasets from human foetal brain tissue (Figure 4C), alongside in vitro differentiation models using human induced pluripotent stem cell (hiPSC)-derived cortical organoids (Figure 4D) and the BrainSpan dataset (Figure 4E). In developing human brain tissue, *SLC39A8* expression was highest in vascular cell types, with peak expression observed during infancy (Figure 4C). Consistent with these findings, longitudinal expression profiles from both hiPSC-derived cortical spheroids and the BrainSpan human developmental transcriptome atlas demonstrated a progressive increase in *SLC39A8* expression across developmental stages (Figure 3D-E). Expression was lowest during early embryonic stages, increasing steadily through mid-gestation and infancy, and reaching maximal levels during postnatal development. Together, these data suggest that rs13107325 may exert its influence during a critical window of brain maturation, potentially linking synaptic and neurovascular development with later vulnerability to psychiatric and metabolic illness.

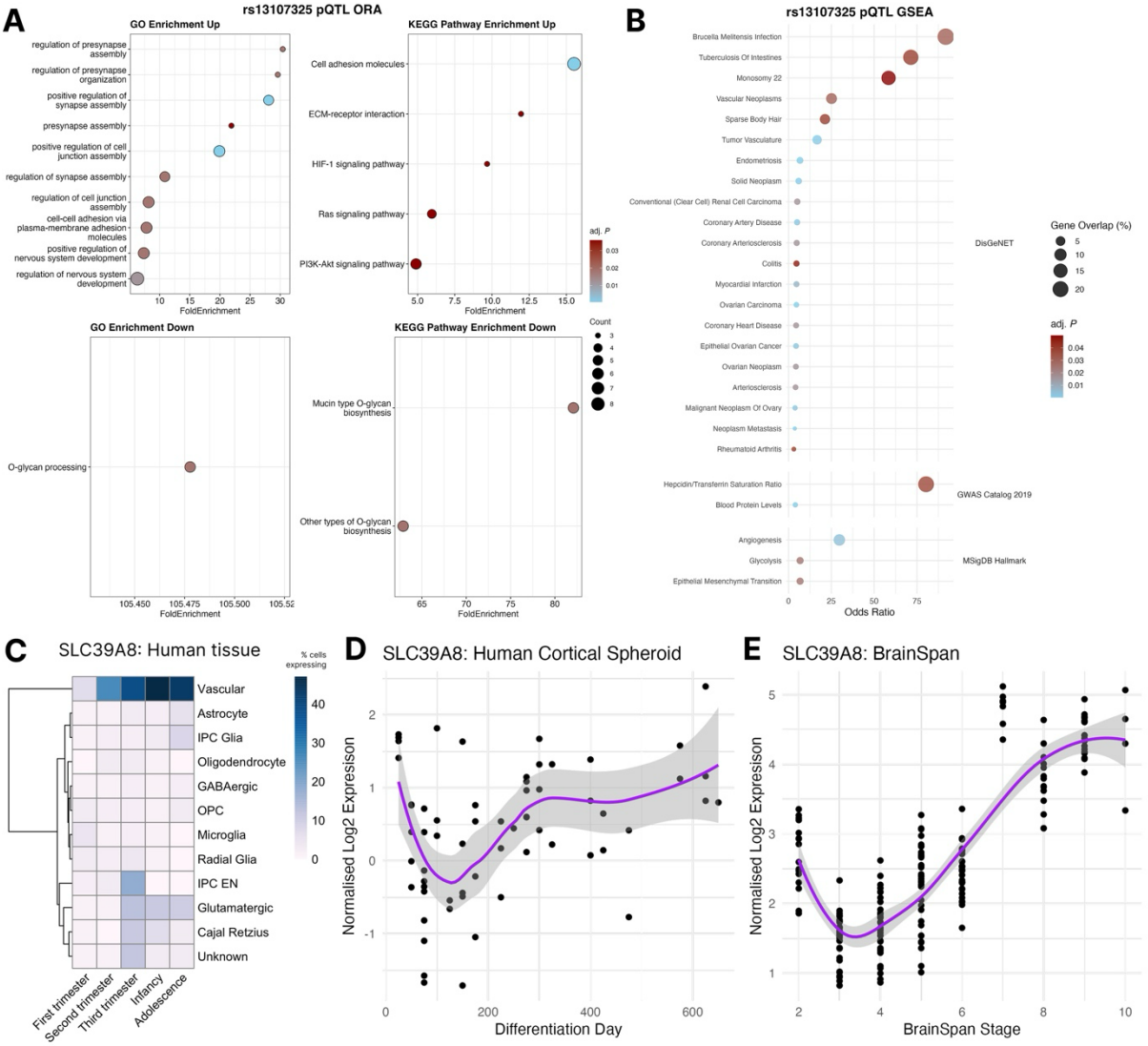

Figure 4: *Pathway analysis of rs13107325 pQTLs and developmental expression of SLC39A8 (A) Over-representation analysis (ORA) of genes whose protein levels are associated with the rs13107325 variant. GO biological process terms (left panels) and KEGG pathways (right panels) are shown for proteins upregulated (top) or downregulated (bottom) with the minor allele. Dot size represents gene ratio; colour represents adjusted p-value. (B) Gene set enrichment analysis (GSEA) of rs13107325 pQTLs using DisGeNET, GWAS Catalog, and MSigDB hallmark gene sets. Dot size reflects gene overlap percentage; colour reflects adjusted p-value; x-axis indicates odds ratio. (C) Heatmap showing percentage of cells expressing SLC39A8 across different human brain cell types and developmental stages, data from publicly available scRNA-seq [31]. SLC39A8 is most strongly expressed in vascular cells, peaking in infancy. (D) Temporal expression profile of SLC39A8 in human cortical spheroids across differentiation time, with data from publicly available bulk-RNAseq [32]. Data represent normalized log2 expression values with a LOESS regression fit and 95% confidence interval. (E) SLC39A8 expression in the human brain across developmental stages in the BrainSpan dataset [33]; RNA sequencing and exon microarray data profiling of up to sixteen cortical and subcortical*

structures across the full course of human brain development. Developmental stages are: early prenatal (8–10 post-conceptional weeks [PCW], Stage 2), mid prenatal (10–13 PCW, Stage 3; 13–16 PCW, Stage 4; 16–19 PCW, Stage 5; 19–24 PCW, Stage 6), late prenatal (24–38 PCW, Stage 7), early infancy (birth–6 months, Stage 8), late infancy (6–19 months, Stage 9), early childhood (19 months–5 years, Stage 10), middle childhood (6–11 years, Stage 11), adolescence (12–19 years, Stage 12), and young adulthood (21–40 years, Stage 13). Expression values are normalized log_2 values with LOESS smoothing and 95% confidence interval.

Discussion

Our multi-trait colocalization analysis revealed a shared genetic risk loci between SZ, TG:HDL-C, bilateral CT and plasma IL-6ST at the rs13107325 variant in *SLC39A8*. Further loci identified robust intersections between SZ and IL-6R (rs2853986), SZ and TG:HDL-C (rs6765484 and rs881844). Clusters of SZ with IL6ST, FI, LH-CT (rs4240624), and L/RH-CT were unstable past default thresholds.

Together, these results present one novel shared causal variant that may underpin pleiotropic effects relevant to neuropsychiatric and immuno-metabolic disease risk: rs13107325. This *SLC39A8* missense variant related brain structure, insulin resistance and IL-6 signalling traits to SZ with stability across sensitivity analyses, maintaining strong colocalization even under stringent priors and thresholds. Previous colocalization work has clustered this SNP with SZ, high-density lipoprotein (HDL), triglycerides (TG), body mass index (BMI), and type-2 diabetes [36]. We extend this work to demonstrate its colocalization with brain structure and IL-6 signalling. In the UK Biobank general population, *SLC39A8*^{A939T} has been associated with poorer cognitive performance [37]. In rodent models that contain SLC39A8-p.393T, corresponding to rs13107325 (p.Ala391Thr), have been shown to have reduced increased Zn^{2+} blood levels, decreased Zn^{2+} levels in the cortex and reduced dendritic spine density in the somatosensory/motor cortex compared with wild type controls, suggesting an impact of this variant on the development of neuronal connectivity [38]. In addition, *SLC39A8*$^{+/-}$ mice had reduced blood-brain barrier integrity and elevated plasma IL-6 and IL-1β expression after bacterial endotoxin lipopolysaccharide (LPS) treatment compared with wild type controls [39]. Further *in vitro* studies using

rodent immortalised and primary cell lines have shown this variant to disrupt excitatory neurotransmission by reducing glutamate receptor surface expression and impairing zinc regulation in the synaptic cleft [39]. Plus, *SLC39A8*^{A939T} in HEK293 cells heightened NFκB activation following TNFα stimulation [39]. Finally, individuals with early schizophrenia (SZ) exhibit an increased brain age gap, where sMRI-estimated brain age exceeds chronological age [40–42]. Recently, SLC39A8 expression was found to be significantly associated with a brain ageing pattern defined by reduced grey matter thickness in the prefrontal, parietal, and temporal cortices—regions consistently implicated in both SZ and cognitive decline [43]. This imaging-derived phenotype, linked to SLC39A8 expression, also correlated with non-imaging markers such as BMI, weight, red blood cell count, and head bone mineral density, suggesting a connection between brain ageing and broader physiological dysregulation [43]. Overall, observations resonate with an emerging hypothesis that advanced or accelerated brain ageing caused by metabolic dysfunction [44,45] may underlie vulnerability to psychosis. If rs13107325 is affecting risk at developmental stages, this suggests potential unifying explanation for how metabolic risk, inflammation, abnormal brain structure co-occur in schizophrenia.

Our expression and pathway analysis demonstrated temporal, cellular and functional contexts of rs13107325 that further supports a developmental window of vulnerability for this pleiotropic mechanism. Our analysis of publicly available transcriptomic data indicates that SLC39A8 expression is highest in vascular cells of the developing brain, with increasing expression from embryogenesis through infancy [31]. This expression trajectory was recapitulated in both iPSC-derived organoid and BrainSpan datasets [32,33]. Supporting this, previous work suggests that SLC39A8 expression is enriched in brain endothelial cells compared to peripheral systems, indicating a potentially more integral role for the transporter in the brain vasculature [39,46]. The enrichment of rs13107325-associated pQTLs in synapse developmental pathways further supports a model in which this variant may exert its effects during key periods of maturation. Complementing this, GSEA identified an enrichment for glycolysis, indicating that disruption of SLC39A8-mediated metal transport could have cascading effects on cellular metabolism and synapse development during vulnerable periods.

Given the role of SLC39A8 in metal ion transport, the rs13107325 variant may disrupt brain development either directly, by reducing ion influx into the brain, or indirectly, through downstream effects on protein expression required for neuronal maturation and synaptic function. Our colocalization results, in combination with ORA/GSEA pathway enrichment results from the variants' pQTLs, demonstrate the potential involvement of rs13107325 in immuno-metabolic pathways with impacts on energy metabolism and inflammatory signalling during development. SLC39A8 is highly expressed in endothelial cells during early life [31], raising the possibility that its dysfunction compromises blood–brain barrier (BBB) integrity during infancy [39], a period when the barrier is still forming and particularly susceptible to damage. IL-6 plays a critical role in brain development, regulating processes such as neuronal differentiation, growth, and survival [47]. IL-6 trans-signalling is buffered by soluble gp130 (IL-6ST), which binds the IL-6:sIL-6R complex with high affinity to prevent excessive pro-inflammatory signalling [11]. Elevated plasma IL-6ST, for which rs13107325 is associated, may thus reflect increased capacity to dampen IL-6-mediated inflammation, thereby weakening the buffer system. When coupled with a leaky BBB, this may result in either chronically unregulated inflammatory pathways, or a failure to engage developmentally essential IL-6-dependent pathways, both of which could increase vulnerability to schizophrenia during brain development. These findings suggest testable mechanisms by which metal ion transport, dyslipidaemia, and inflammation may converge to shape early brain and vascular development and prime long-term psychiatric risk.

Beyond rs13107325 and SLC39A8 dysfunction, robust colocalization between schizophrenia and plasma IL-6R at the rs2853986 locus remained stable across sensitivity analyses. This variant is in an intergenic region corresponding to the Major Histocompatibility Complex (MHC) Class I region (6p21.33), the genomic area conveying the greatest risk for schizophrenia [25]. These findings support the hypothesis that inflammatory pathways, particularly those involving adaptive immunity and IL-6 trans-signalling via soluble IL-6R in the blood, are potentially causally related to psychiatric disorders [13,48–50].

This study has several strengths and limitations that should be acknowledged. It benefits from the use of large-scale GWAS summary statistics from well-powered consortia, enabling robust identification of shared genetic loci through stringent colocalization methods and extensive sensitivity analyses. By applying HyPrColoc, the analysis moves beyond genome-wide correlations to pinpoint specific variants with pleiotropic effects across schizophrenia, brain structure, insulin resistance, and inflammation. However, weaknesses and remaining challenges should be acknowledged. First, although colocalization identifies regions of shared genetic risk, this method cannot determine the direction of causality or underlying mechanisms. For example, although loci such as rs13107325 influence multiple phenotypes, it remains unclear whether immune-metabolic dysfunction drives neurodevelopmental changes leading to schizophrenia, or vice versa. Mendelian randomization and functional *in vitro* or *in vivo* studies are needed to clarify these relationships. Secondly, despite integrating diverse datasets, the study is limited by its reliance on GWAS data from European ancestry samples, which restricts generalisability and fails to capture potential ancestry-specific effects. Finally, the use of proxy measures for complex traits also constrains interpretability. Future studies incorporating greater representation in data and experimental validation of causality will be critical to advance these findings and their clinical relevance.

Conclusion

In summary, this study provides novel compelling evidence for a shared genetic risk variant implicated across schizophrenia, brain structure, insulin resistance and inflammation. Through multi-trait colocalization analysis, we identified robust colocalization at two loci. First, with the missense variant rs13107325 in SLC39A8 emerging as a potential key candidate conveying risk for schizophrenia, thinner bilateral cortical thickness, elevated TG:HDL-C, elevated plasma IL-6ST. Second, with the MHC-region locus rs2853986, conveying risk for both SZ and elevated IL-6R. Our findings suggest that impaired SLC39A8-mediated metal ion transport may represent one convergent biological mechanism underlying the multimorbidity frequently observed in schizophrenia, encompassing metabolic and

inflammatory pathways as well as developmental processes. These results underscore the importance of considering pleiotropic genetic effects in the aetiology of psychotic disorders and their physical health comorbidities. Future studies including for example employing Mendelian randomisation, and in vitro functional assays will be essential to clarify causal relationships and to explore the therapeutic targeting metal ion transport pathways in mitigating both psychiatric and somatic disease burden.

Acknowledgements

This research is supported by the NIHR Oxford Health Biomedical Research Centre. The views expressed are those of the author(s) and not necessarily those of the NIHR or the Department of Health and Social Care.

References

1. Palmer, E. R. *et al.* Trajectories of Inflammation in Youth and Risk of Mental and Cardiometabolic Disorders in Adulthood. *JAMA Psychiatry* **81**, 1130–1137 (2024).

2. Owen, M. J., Legge, S. E., Rees, E., Walters, J. T. R. & O'Donovan, M. C. Genomic findings in schizophrenia and their implications. *Mol Psychiatry* **28**, 3638 (2023).

3. Andreazza, A. C. *et al.* Brain and body energy metabolism and potential for treatment of psychiatric disorders. *Nature Mental Health 2025* 1–9 (2025) doi:10.1038/s44220-025-00422-6.

4. Pillinger, T., D'Ambrosio, E., McCutcheon, R. & Howes, O. D. Is psychosis a multisystem disorder? A meta-review of central nervous system, immune, cardiometabolic, and endocrine alterations in first-episode psychosis and perspective on potential models. *Mol Psychiatry* **24**, 776–794 (2019).

5. Perry, B. I. *et al.* Dysglycaemia, Inflammation and Psychosis: Findings From the UK ALSPAC Birth Cohort. *Schizophr Bull* **45**, 330–338 (2019).

6. Perry, B. I., McIntosh, G., Weich, S., Singh, S. & Rees, K. The association between first-episode psychosis and abnormal glycaemic control: systematic review and meta-analysis. *Lancet Psychiatry* **3**, 1049–1058 (2016).

7. Upthegrove, R., Manzanares-Teson, N. & Barnes, N. M. Cytokine function in medication-naive first episode psychosis: a systematic review and meta-analysis. *Schizophr Res* **155**, 101–108 (2014).

8. Corsi-Zuelli, F. *et al.* Depressive and Negative Symptoms in the Early and Established Stages of Schizophrenia: Integrating Structural Brain Alterations, Cognitive Performance, and Plasma Interleukin 6 Levels. *Biological psychiatry global open science* **5**, (2024).

9. Lalousis, P. A. *et al.* Anhedonia as a Potential Transdiagnostic Phenotype With Immune-Related Changes in Recent-Onset Mental Health Disorders. *Biol Psychiatry* **96**, 615–622 (2024).

10. Lalousis, P. A. *et al.* Inflammatory subgroups of schizophrenia and their association with brain structure: A semi-supervised machine learning examination of heterogeneity. *Brain Behav Immun* **113**, 166–175 (2023).

11. Rose-John, S., Jenkins, B. J., Garbers, C., Moll, J. M. & Scheller, J. Targeting IL-6 trans-signalling: past, present and future prospects. *Nature Reviews Immunology 2023 23:10* **23**, 666–681 (2023).

12. Reeh, H. *et al.* Response to IL-6 trans- A nd IL-6 classic signalling is determined by the ratio of the IL-6 receptor α to gp130 expression: Fusing experimental insights and dynamic modelling. *Cell Communication and Signaling* **17**, 1–21 (2019).

13. González-Castro, T. B. *et al.* Effects of IL-6/IL-6R axis alterations in serum, plasma and cerebrospinal fluid with the schizophrenia: an updated review and meta-analysis of 58 studies. *Mol Cell Biochem* **479**, 525–537 (2024).

14. Van Haren, N. E. M. *et al.* Changes in Cortical Thickness During the Course of Illness in Schizophrenia. *Arch Gen Psychiatry* **68**, 871–880 (2011).

15. Hulshoff Pol, H. E. *et al.* Volume changes in gray matter in patients with schizophrenia. *American Journal of Psychiatry* **159**, 244–250 (2002).

16. Wang, H. *et al.* Shared genetic architecture of cortical thickness alterations in major depressive disorder and schizophrenia. *Prog Neuropsychopharmacol Biol Psychiatry* **135**, (2024).

17. Cheng, W. *et al.* Genetic Association between Schizophrenia and Cortical Brain Surface Area and Thickness. *JAMA Psychiatry* **78**, 1020–1030 (2021).

18. Williams, J. A. *et al.* Inflammation and Brain Structure in Schizophrenia and Other Neuropsychiatric Disorders: A Mendelian Randomization Study. *JAMA Psychiatry* **79**, 498–507 (2022).

19. Kirschner, M. *et al.* Schizophrenia Polygenic Risk During Typical Development Reflects Multiscale Cortical Organization. *Biological Psychiatry Global Open Science* **3**, 1083–1093 (2023).

20. Meyer, U. Neurodevelopmental Resilience and Susceptibility to Maternal Immune Activation. *Trends Neurosci* **42**, 793–806 (2019).

21. Allswede, D. M., Yolken, R. H., Buka, S. L. & Cannon, T. D. Cytokine concentrations throughout pregnancy and risk for psychosis in adult offspring: a longitudinal case-control study. *Lancet Psychiatry* **7**, 254–261 (2020).

22. Rudolph, M. D. *et al.* Maternal IL-6 during pregnancy can be estimated from newborn brain connectivity and predicts future working memory in offspring. *Nat Neurosci* **21**, 765–772 (2018).

23. Rasmussen, J. M. *et al.* Maternal Interleukin-6 concentration during pregnancy is associated with variation in frontolimbic white matter and cognitive development in early life. *Neuroimage* **185**, 825–835 (2019).

24. Smith, S. E. P., Li, J., Garbett, K., Mirnics, K. & Patterson, P. H. Maternal immune activation alters fetal brain development through interleukin-6. *Journal of Neuroscience* **27**, 10695–10702 (2007).

25. Trubetskoy, V. *et al.* Mapping genomic loci implicates genes and synaptic biology in schizophrenia. *Nature 2022 604:7906* **604**, 502–508 (2022).

26. Smith, S. M. *et al.* An expanded set of genome-wide association studies of brain imaging phenotypes in UK Biobank. *Nat Neurosci* **24**, 737–745 (2021).

27. Oliveri, A. *et al.* Comprehensive genetic study of the insulin resistance marker TG:HDL-C in the UK Biobank. *Nat Genet* **56**, 212–221 (2024).

28. Lotta, L. A. *et al.* Integrative genomic analysis implicates limited peripheral adipose storage capacity in the pathogenesis of human insulin resistance. *Nat Genet* **49**, 17–26 (2017).

29. Sun, B. B. *et al.* Plasma proteomic associations with genetics and health in the UK Biobank. *Nature 2023 622:7982* **622**, 329–338 (2023).

30. Foley, C. N. *et al.* A fast and efficient colocalization algorithm for identifying shared genetic risk factors across multiple traits. *Nature Communications 2021 12:1* **12**, 1–18 (2021).

31. Wang, L. *et al.* Molecular and cellular dynamics of the developing human neocortex. *Nature 2025* 1–10 (2025) doi:10.1038/s41586-024-08351-7.

32. Gordon, A. *et al.* Long-term maturation of human cortical organoids matches key early postnatal transitions. *Nat Neurosci* **24**, 331–342 (2021).

33. Miller, J. A. *et al.* Transcriptional landscape of the prenatal human brain. *Nature 2014 508:7495* **508**, 199–206 (2014).

34. Carrera, N. *et al.* Association study of nonsynonymous single nucleotide polymorphisms in schizophrenia. *Biol Psychiatry* **71**, 169–177 (2012).

35. Choi, E. K., Nguyen, T. T., Gupta, N., Iwase, S. & Seo, Y. A. Functional analysis of SLC39A8 mutations and their implications for manganese deficiency and mitochondrial disorders. *Scientific Reports 2018 8:1* **8**, 1–17 (2018).

36. Perry, B. I. *et al.* Evidence for Shared Genetic Aetiology Between Schizophrenia, Cardiometabolic, and Inflammation-Related Traits: Genetic Correlation and Colocalization Analyses. *Schizophr Bull Open* **3**, (2022).

37. Smart, S. E. *et al.* SLC39A8.p.(Ala391Thr) is associated with poorer cognitive ability: a cross-sectional study of schizophrenia and the general UK population. *medRxiv* 2024.09.18.24313865 (2024) doi:10.1101/2024.09.18.24313865.

38. Li, S. *et al.* The schizophrenia-associated missense variant rs13107325 regulates dendritic spine density. *Transl Psychiatry* **12**, 361 (2022).

39. Tseng, W. C. *et al.* Schizophrenia-associated SLC39A8 polymorphism is a loss-of-function allele altering glutamate receptor and innate immune signaling. *Translational Psychiatry 2021 11:1* **11**, 1–11 (2021).

40. Constantinides, C. *et al.* Brain ageing in schizophrenia: evidence from 26 international cohorts via the ENIGMA Schizophrenia consortium. *Mol Psychiatry* **28**, 1201–1209 (2023).

41. Hua, J. P. Y. *et al.* Brain Age Gap in Early Illness Schizophrenia and the Clinical High-Risk Syndrome: Associations With Experiential Negative Symptoms and Conversion to Psychosis. *Schizophr Bull* **50**, 1159–1170 (2024).

42. Murray, A. J. *et al.* Probing the Biological Underpinnings of Advanced Brain Ageing in Schizophrenia. *medRxiv* 2024.07.05.24309965 (2024) doi:10.1101/2024.07.05.24309965.

43. Smith, S. M. *et al.* Brain aging comprises many modes of structural and functional change with distinct genetic and biophysical associations. *Elife* **9**, (2020).

44. Murray, A. J., Rogers, J. C., Katshu, M. Z. U. H., Liddle, P. F. & Upthegrove, R. Oxidative Stress and the Pathophysiology and Symptom Profile of Schizophrenia Spectrum Disorders. *Front Psychiatry* **12**, 703452 (2021).

45. Koutsouleris, N. *et al.* BMIgap: a new tool to quantify transdiagnostic brain signatures of current and future weight. *Res Sq* (2024) doi:10.21203/RS.3.RS-5259910/V1.

46. Zhang, Y. *et al.* An RNA-sequencing transcriptome and splicing database of glia, neurons, and vascular cells of the cerebral cortex. *Journal of Neuroscience* **34**, 11929–11947 (2014).

47. Kummer, K. K., Zeidler, M., Kalpachidou, T. & Kress, M. Role of IL-6 in the regulation of neuronal development, survival and function. *Cytokine* **144**, 155582 (2021).

48. Giollabhui, N. Mac *et al.* Role of Inflammation in Depressive and Anxiety Disorders, Affect, and Cognition: Genetic and Non-Genetic Findings in the Lifelines Cohort Study. *Res Sq* (2024) doi:10.21203/RS.3.RS-4379779/V1.

49. Milaneschi, Y. *et al.* Association of inflammation with depression and anxiety: evidence for symptom-specificity and potential causality from UK Biobank and NESDA cohorts. *Mol Psychiatry* **26**, 7393–7402 (2021).

50. Ferreira, R. C. *et al.* Functional IL6R 358Ala allele impairs classical IL-6 receptor signaling and influences risk of diverse inflammatory diseases. *PLoS Genet* **9**, (2013).